

Quantum search of many vertices on the joined complete graph

Tingting Ji(冀婷婷), Naiqiao Pan(潘乃桥), Tian Chen(陈天), and Xiangdong Zhang(张向东)
Citation: Chin. Phys. B, 2022, 31 (**7**): 070504. DOI: 10.1088/1674-1056/ac5241
Journal homepage: http://cpb.iphy.ac.cn; http://iopscience.iop.org/cpb

What follows is a list of articles you may be interested in

Nonlinear dynamics of cell migration in anisotropic microenvironment

Yanping Liu(刘艳平), Da He(何达), Yang Jiao(焦阳), Guoqiang Li(李国强), Yu Zheng(郑钰), Qihui Fan(樊琪慧), Gao Wang(王高), Jingru Yao(姚静如), Guo Chen(陈果), Silong Lou(娄四龙), and Liyu Liu(刘雳宇)
Chin. Phys. B, 2021, 30 (**9**): 090505. DOI: 10.1088/1674-1056/ac11d5

Quantum dynamics on a lossy non-Hermitian lattice

Li Wang(王利), Qing Liu(刘青), and Yunbo Zhang(张云波)
Chin. Phys. B, 2021, 30 (**2**): 020506. DOI: 10.1088/1674-1056/abd765

Probe of topological invariants using quantum walks of a trapped ion in coherent state space

Ya Meng(蒙雅), Feng Mei(梅锋), Gang Chen(陈刚), Suo-Tang Jia(贾锁堂)
Chin. Phys. B, 2020, 29 (**7**): 070501. DOI: 10.1088/1674-1056/ab8893

Ergodicity recovery of random walk in heterogeneous disordered media

Liang Luo(罗亮), Ming Yi(易鸣)
Chin. Phys. B, 2020, 29 (**5**): 050503. DOI: 10.1088/1674-1056/ab8212

Quantum walks with coins undergoing different quantum noisy channels

Hao Qin(秦豪) and Peng Xue(薛鹏)
Chin. Phys. B, 2016, 25 (**1**): 010501. DOI: 10.1088/1674-1056/25/1/010501

Quantum search of many vertices on the joined complete graph

Tingting Ji(冀婷婷), Naiqiao Pan(潘乃桥), Tian Chen(陈天)†, and Xiangdong Zhang(张向东)

Key Laboratory of Advanced Optoelectronic Quantum Architecture and Measurements of Ministry of Education, Beijing Key Laboratory of Nanophotonics & Ultrafine Optoelectronic Systems, School of Physics, Beijing Institute of Technology, Beijing 100081, *China*

(Received 24 October 2021; revised manuscript received 29 December 2021; accepted manuscript online 7 February 2022)

The quantum search on the graph is a very important topic. In this work, we develop a theoretic method on searching of single vertex on the graph [*Phys. Rev. Lett.* **114** 110503 (2015)], and systematically study the search of many vertices on one low-connectivity graph, the joined complete graph. Our results reveal that, with the optimal jumping rate obtained from the theoretical method, we can find such target vertices at the time $O\left(\sqrt{N}\right)$, where N is the number of total vertices. Therefore, the search of many vertices on the joined complete graph possessing quantum advantage has been achieved.

Keywords: quantum search, the joined complete graph, quantum walk, many vertices

PACS: 05.40.Fb, 03.67.–a, 02.10.Ox **DOI:** 10.1088/1674-1056/ac5241

1. Introduction

The search problem concerns about the finding of the target data point in one unsorted database. When the number of the data point is N, the success probability to find the target data point is $1/N$ with one random guess. So the average times of queries in finding the target data point is $N/2$, which includes one time of query in the best case and N times of queries in the worst case. The Grover algorithm was firstly proposed as a discrete-time algorithm, which can be described as a method of searching N unsorted databases in times of queries $O\left(\sqrt{N}\right)$.[1–3] Given a black-box function $f(x):\{1,\ldots,N\}\to\{0,1\}$ satisfying $f(x)=\begin{cases}0, x\neq w,\\ 1, x=w,\end{cases}$ the Grover algorithm can find the target w that makes the function value equal to 1 in time $O\left(\sqrt{N}\right)$. A modified Grover algorithm improves the success probability to 1, which has the better performance than that of the original algorithm.[2,3] The Grover algorithm can be used not only for combinatorial search, but also as a subroutine of various other quantum algorithms.[4,5] The experimental studies of such quantum search algorithm have also been provided.[6–10]

Although the Grover algorithm has achieved great success in the quantum search problem, the direct application of this algorithm in physical databases, e.g., the graph structure, cannot work well. In many circumstances, the relations among these physical databases are described by the Hamiltonians. Some efforts have been devoted to applying the Grover algorithm to such databases, but the evolutions governed by these Hamiltonians cannot be easily designed as the requirements of the Grover algorithm. In order to realize the fast quantum search in physical databases described by the Hamiltonians, Childs and Goldstone proposed a graph-based continuous-time quantum walk search algorithm.[11] Random walk is widely employed in designing the classical algorithms, so it is natural to extend the algorithm of random walk from classic to quantum version. The studies of the quantum algorithms based on the graphs have attracted lots of attention.[12–19] Quantum algorithms based on continuous-time quantum walks have revealed an exponential acceleration that surpasses any classical algorithm in solving a certain black-box problem, and can provide a corresponding framework for designing new algorithms, modeling quantum transmission and state transition problems.[20–33] Considering that the graph structure can represent different connections between the vertices, the quantum search algorithms on the graph are also very important. The viewpoint about the success of searching the vertices in the graph depending on the connectivity in the graph lasted over one decade.[34,35] Recent researches point out that through the design of the jumping rate between the adjacent vertices in the graph, the quantum search of the target vertex can be realized in the low-connectivity graphs, which exhibits the quantum advantage over the classical algorithm.[36–40] In these works, the researchers concern about the searching one vertex and such vertex does not locate at the "specific" position (i.e., not on the positions with different connectivity).

In our work, we study the quantum search on one low-connectivity graph-the joined complete graph. The number of target vertices is not limited to one. Our results reveal that, when the target vertices have the same connectivity, the time to reach the maximum success probability has the same expression as that of searching one vertex. When the target vertices have different connectivity, the time to reach the maximum success probability is different from that of searching one vertex. We show that, the times to reach the maximum success probability for different cases belong to $O\left(\sqrt{N}\right)$, where N is the number of total vertices. Therefore, such quantum search algorithms also display the quantum advantage.

In the following, we firstly provide different cases in

†Corresponding author. E-mail: chentian@bit.edu.cn

© 2022 Chinese Physical Society and IOP Publishing Ltd

which the target vertices locate at different positions. Then, we derive and show the general expressions for quantum search in these cases. Graphs with different numbers of vertices are presented to verify the success of quantum search. We conclude at the end of this paper.

2. General descriptions of the joined complete graph

The joined complete graph is addressed below (Fig. 1), which contains N vertices. There are $N/2$ vertices in the left complete graph and the other $N/2$ vertices belong to the right complete graph. The degree of jth vertex $(\deg(j))$ is defined as the number of connecting vertices. So it is clear that the vertices in red, blue, gray and white have the same degrees, but the vertices in yellow and green have the same degrees, which are not the same as above.

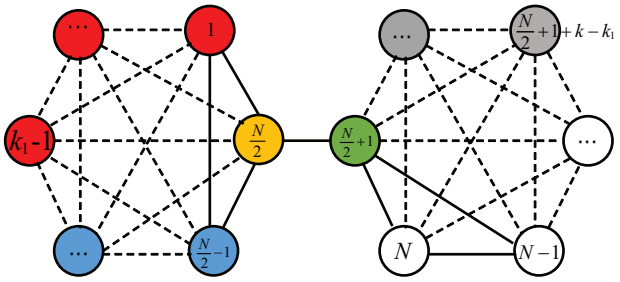


Fig. 1. The schematic representation of the joined complete graph. The vertices in red, blue, gray and white have the same degree $\deg(j)$. The yellow (green) vertex that connect to the other complete graph has different degree. In our discussions, the target vertices may be the red, gray, yellow and green ones. The detailed study is addressed below.

To describe the quantum dynamics of these N vertices, we can use the N dimensional basis $\{|1\rangle, |2\rangle, \ldots, |N\rangle\}$ in the Hilbert space. The jth vertex is expressed as a N dimensional column vector $|j\rangle = (0, \ldots, 1, \ldots, 0)^{\mathrm{T}}$ with the jth element is non-zero. The superscript T represents the transposition operation. The Laplacian matrix $L = D - A$ where the diagonal degree matrix is expressed as D. The element in D is $D_{j,j} = \deg(j)$. The adjacent matrix A describes the connection between vertices in the graph. When the jth vertex is (not) connected to the qth vertex, the corresponding element in the matrix $A_{j,q} = 1\,(0)$. The time-independent Hamiltonian to describe the connection among such joined complete graph can be expressed as γL. The parameter γ represents the jumping rate of the particle from one vertex to another vertex.

In the quantum search problem, the oracle is able to distinguish the "target" and "not-target" vertices. The oracle Hamiltonian $H_j = -|j\rangle\langle j|$ is introduced to highlight the special characteristics of target vertex expressed as $|j\rangle$.[11,34–40] For the state $|j\rangle$, this external potential field $-|j\rangle\langle j|$ is applied; no external fields for other states. In the studies before,[11,34–40] the researchers focused on the search of single vertex, so the number of target vertices k is one. In our study here, we pay attention to the search of many vertices, so the number of target vertices k is larger than one, but still far smaller than the number of total vertices N. To reveal the effect of the oracle, the external fields are also applied on these k vertices. The corresponding oracle Hamiltonian is expressed as $-\sum_{j\in\text{marked}}^{j=1,\ldots,k} |j\rangle\langle j|$. The total time-independent Hamiltonian for the quantum search in the joined complete graph can be expressed as $H = \gamma L - \sum_{j\in\text{marked}}^{j=1,\ldots,k} |j\rangle\langle j|$. When the number of vertices is large enough (it is commonly seen in the realistic search scene), the elements in D are viewed the same and the effect of D can be safely neglected when deriving the optimal jumping rate. Therefore, the Hamiltonian changes to $H = -\gamma A - \sum_{j\in\text{marked}}^{j=1,\ldots,k} |j\rangle\langle j|$. In the quantum search problem of the graph, we aim to find the optimal jumping rate and realize the search of target vertices in a short time. The initial state in the search process is assumed as $|s\rangle = \frac{1}{\sqrt{N}} \sum_{j}^{j=1,\ldots,N} |j\rangle = \frac{1}{\sqrt{N}}(1, 1, \ldots, 1, 1)^{\mathrm{T}}$ which means no knowledge about the target vertices. When the target vertices belong to the red, yellow, green and gray ones, the success probabilities are totally different. In the following, we will discuss the quantum search of many target vertices in the joined complete graph in detail.

3. The quantum search of many vertices in the joined complete graph

The positions of target vertices can be grouped into several different cases. In the below, we will provide the derivation of optimal jumping rate in each case and verify the success of the quantum search of these target vertices. As shown in Fig. 1, the joined complete graph is composed by one complete graph in the left and the other complete graph in the right. Therefore, the successful search with the maximum probability relies on the distribution of the target vertices. If target vertices are all located at the left or right complete graph, the successful search is defined as the search probability of target vertices being very close to 1/2. This value 1/2 results from the low connectivity between the left and right complete graphs. The evolution of search starts from the equal superposition of all vertices. In the search process, when the target vertices are only located on one complete graph, the probabilities on the other complete graph cannot fully flow into the adjacent complete graph by going through the only one connection between these two complete graphs. The simplest case is finding only one vertex in the joined complete graph.[35] As the target vertex is only on one of the complete graphs, the successful search is defined with the probability of finding the target vertex as 1/2. In comparison, if some target vertices are located at the left and the others are located at the right complete graph,

the successful search is defined as the search probability of target vertices being very close to 1. In this scenario, the probabilities on each complete graph are accumulated to the target vertices on the corresponding graph during the search process.

In realistic conditions, the number of target vertices k is commonly far smaller than the number of total vertices N. In our discussion, we assume such condition is satisfied in all cases.

3.1. All the target vertices are red ones

Here, we study the case when k target vertices are all red ones. In this case, all the target vertices are located on the left complete graph. All vertices are grouped according to the connectivity on the graph. The target vertices are grouped together, and the other vertices can be grouped based on the connection with the target vertices and the location on the graph. The reason to group all vertices into different categories is for finding the optimal value of γ conveniently. The details are addressed below. In this case, the vertices in gray and white in the right complete graph can be seen as the vertices possessing the same properties. According to the method shown in Ref. [35], we can group the N vertices into five categories as

$$\begin{aligned}
&|a\rangle = \frac{1}{\sqrt{k}} \sum_{j\in\text{red}} |j\rangle, \quad |b\rangle = \frac{1}{\sqrt{\frac{N}{2}-k-1}} \sum_{j\in\text{blue}} |j\rangle,\\
&|c\rangle = |\text{yellow}\rangle, \quad |d\rangle = |\text{green}\rangle,\\
&|e\rangle = \frac{1}{\sqrt{\frac{N}{2}-1}} \sum_{\substack{j\in\text{gary}\\ \&\text{white}}} |j\rangle. \qquad (1)
\end{aligned}$$

In Eq. (1), the "yellow" and "green" in "$|\ \rangle$" represent the vertices in yellow and green colors in Fig. 1, respectively. The vertex in yellow is the $\frac{N}{2}$th vertex in the graph, and the state is $|\text{yellow}\rangle = \left|\frac{N}{2}\right\rangle$. The vertex in green is the $\left(\frac{N}{2}+1\right)$th vertex in the graph, and the state is $|\text{green}\rangle = \left|\frac{N}{2}+1\right\rangle$. The Hamiltonian H can be expanded by these five bases (Eq. (1)) as

$$H = -\gamma \begin{pmatrix}
k-1+\frac{1}{\gamma} & \sqrt{k(\frac{N}{2}-k-1)} & \sqrt{k} & 0 & 0\\
\sqrt{k(\frac{N}{2}-k-1)} & \frac{N}{2}-k-2 & \sqrt{\frac{N}{2}-k-1} & 0 & 0\\
\sqrt{k} & \sqrt{\frac{N}{2}-k-1} & 0 & 1 & 0\\
0 & 0 & 1 & 0 & \sqrt{\frac{N}{2}-1}\\
0 & 0 & 0 & \sqrt{\frac{N}{2}-1} & \frac{N}{2}-2
\end{pmatrix}. \qquad (2)$$

When the number of target vertices k is commonly far smaller than the number of total vertices N, we simplify H to

$$H = -\gamma \begin{pmatrix}
\frac{1}{\gamma} & \sqrt{\frac{kN}{2}} & \sqrt{k} & 0 & 0\\
\sqrt{\frac{kN}{2}} & \frac{N}{2} & \sqrt{\frac{N}{2}} & 0 & 0\\
\sqrt{k} & \sqrt{\frac{N}{2}} & 0 & 1 & 0\\
0 & 0 & 1 & 0 & \sqrt{\frac{N}{2}}\\
0 & 0 & 0 & \sqrt{\frac{N}{2}} & \frac{N}{2}
\end{pmatrix}. \qquad (3)$$

To find the optimal jumping rate, we can decompose this Hamiltonian in Eq. (3) as $H = H_0 + H_1 + H_2$ where the leading order matrix elements in H_0, H_1 and H_2 are N, $\sqrt{N}$ and 1, respectively. The details of H_0, H_1 and H_2 are addressed as

$$H_0 = -\gamma \begin{pmatrix}
\frac{1}{\gamma} & 0 & 0 & 0 & 0\\
0 & \frac{N}{2} & 0 & 0 & 0\\
0 & 0 & 0 & 0 & 0\\
0 & 0 & 0 & 0 & 0\\
0 & 0 & 0 & 0 & \frac{N}{2}
\end{pmatrix},$$

$$H_1 = -\gamma \begin{pmatrix}
0 & \sqrt{\frac{kN}{2}} & 0 & 0 & 0\\
\sqrt{\frac{kN}{2}} & 0 & \sqrt{\frac{N}{2}} & 0 & 0\\
0 & \sqrt{\frac{N}{2}} & 0 & 0 & 0\\
0 & 0 & 0 & 0 & \sqrt{\frac{N}{2}}\\
0 & 0 & 0 & \sqrt{\frac{N}{2}} & 0
\end{pmatrix},$$

$$H_2 = -\gamma \begin{pmatrix}
0 & 0 & \sqrt{k} & 0 & 0\\
0 & 0 & 0 & 0 & 0\\
\sqrt{k} & 0 & 0 & 1 & 0\\
0 & 0 & 1 & 0 & 0\\
0 & 0 & 0 & 0 & 0
\end{pmatrix}. \qquad (4)$$

When N is large enough, the elements in H_0 are far larger than those in H_1 and H_2, and the elements in H_1 are far larger than those in H_2. So the effect from H_2 can be neglected safely. Considering there is no knowledge about target vertices at the beginning, the initial state of quantum search is

$$\begin{aligned}
|s\rangle = \frac{1}{\sqrt{N}} \sum_j |j\rangle = \frac{\sqrt{k}}{\sqrt{N}} |a\rangle + \frac{\sqrt{\frac{N}{2}-k-1}}{\sqrt{N}} |b\rangle\\
+ \frac{1}{\sqrt{N}} |c\rangle + \frac{1}{\sqrt{N}} |d\rangle + \frac{\sqrt{\frac{N}{2}-1}}{\sqrt{N}} |e\rangle.
\end{aligned}$$

The state $|s\rangle$ is mainly composed by $|b\rangle$ and $|e\rangle$ with large N.

As revealed in Eq. (4), the Hamiltonian H_0 is only spanned by $|a\rangle$, $|b\rangle$ and $|e\rangle$. If the relation $\frac{1}{\gamma}=\frac{N}{2}$ is assumed, the corresponding eigenstates $|a\rangle$, $|b\rangle$ and $|e\rangle$ become degenerated states. When these states $|a\rangle$, $|b\rangle$ and $|e\rangle$ are degenerated, H_1 plays the role as the perturbation to transit the probability from $|b\rangle$ and $|e\rangle$ to $|a\rangle$. During the search process, the probability is accumulated in the state $|a\rangle$, we can find such state with a non-negligible probability and finish the search. If the eigenstates $|a\rangle$, $|b\rangle$ and $|e\rangle$ are non-degenerated, the system evolution will be confined to the initial state, and the probability for the target state $|a\rangle$ will not be large. The terms in H_0+H_1 which describe the connection between $|a\rangle$, $|b\rangle$ and $|e\rangle$ can be re-expressed in one matrix spanned by these three bases as

$$H_0+H_1=\begin{pmatrix} -1 & -\sqrt{\frac{2k}{N}} & 0 \\ -\sqrt{\frac{2k}{N}} & -1 & 0 \\ 0 & 0 & -1 \end{pmatrix}. \tag{5}$$

The eigenstates are $|\varphi_1\rangle=\frac{1}{\sqrt{2}}(|a\rangle+|b\rangle)|\varphi_2\rangle=|e\rangle$ and $|\varphi_3\rangle=\frac{1}{\sqrt{2}}(-|a\rangle+|b\rangle)$, and the corresponding eigenvalues are $E_1=-1-\sqrt{\frac{2k}{N}}$, $E_2=-1$ and $E_3=-1+\sqrt{\frac{2k}{N}}$, respectively. Therefore, the initial state is $|s\rangle=\frac{1}{\sqrt{N}}\sum_j|j\rangle=\frac{\sqrt{k}}{\sqrt{N}}|a\rangle+\frac{\sqrt{\frac{N}{2}-k-1}}{\sqrt{N}}|b\rangle+\frac{1}{\sqrt{N}}|c\rangle+\frac{1}{\sqrt{N}}|d\rangle+\frac{\sqrt{\frac{N}{2}-1}}{\sqrt{N}}|e\rangle$, and it becomes $|s\rangle\approx\frac{1}{\sqrt{2}}(|b\rangle+|e\rangle)=\frac{1}{\sqrt{2}}\left[\frac{1}{\sqrt{2}}(|\varphi_1\rangle+|\varphi_3\rangle)+|\varphi_2\rangle\right]=\frac{1}{2}(|\varphi_1\rangle+|\varphi_3\rangle)+\frac{1}{\sqrt{2}}|\varphi_2\rangle$ when N is large. The target vertices are expressed as $|a\rangle$, and the success amplitude of finding $|a\rangle$ with time is $\langle a|\varphi(t)\rangle=\langle a|\,\mathrm{e}^{-\mathrm{i}(H_0+H_1)t}\,|s\rangle=\frac{1}{\sqrt{2}}\mathrm{e}^{\mathrm{i}t}\mathrm{i}\sin\sqrt{\frac{2k}{N}}t$. So the searching probability of $|a\rangle$ is $p=|\langle a|\,\varphi(t)\rangle|^2=\frac{1}{2}\sin^2\sqrt{\frac{2k}{N}}t$. Our goal in the quantum search is to find these target vertices, which are grouped into the state $|a\rangle$. Therefore, such probability $p=|\langle a|\,\varphi(t)\rangle|^2$ is the success probability in the search process. It is clearly found that the maximum searching probability 1/2 is achieved at time $t=\frac{\pi}{2}\sqrt{\frac{N}{2k}}$, which means the successful search has been realized.

In Fig. 2, we provide the searching results. In Fig. 2(a), we discuss the scenario that the total number of vertices is $N=128$ and the target vertices is $k=5$. The blue line represents the numerical results obtained from the quantum walk evolution under N dimensional Hilbert space, and red dots are depicted from the expression of searching probability p provided above. As revealed from our theoretical derivation, the maximum searching probability 1/2 can be reached at the first time at $t=\frac{\pi}{2}\sqrt{\frac{N}{2k}}\approx 5.62$. The time obtained from the numerical simulation and the theoretical derivation are the same. The only difference between the numerical simulation and the theoretical derivation comes from the beginning of the evolution. For the theoretical derivation assumes that the number of total vertices is rather large. The simulation results and the theoretical derivation agree well in Fig. 2(b), and the maximum searching probability 1/2 can be reached at the first time at $t=\frac{\pi}{2}\sqrt{\frac{N}{2k}}\approx 7.95$. Due to large number of vertices, the difference between the numerical simulation and the theoretical derivation at the beginning of the evolution is smaller than that in Fig. 2(a).

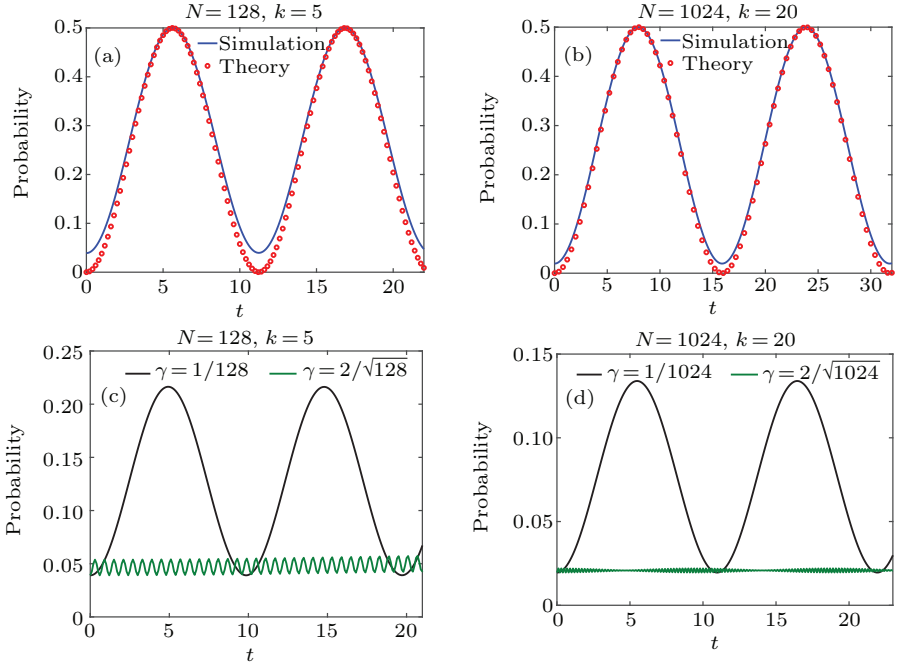


Fig. 2. The success search probability of target vertices in the joined complete graph. In this case, all red vertices in Fig. 1 are target vertices. The total number of vertices in (a) and (b) are 128 and 1024, respectively. The number of target vertices in (a) and (b) are 5 and 20, respectively. The value of $\gamma=2/N$. In two panels, the red dots are the theoretic derivation of probability above. Blue solid lines represent the numerical results obtained by quantum walk evolution under N dimensional Hilbert space. In (c), the black (green) solid line represents the evolution of probability over time when $\gamma=1/N$ ($\gamma=2/\sqrt{N}$) in the model with $N=128$ and $k=5$. In (d), the black (green) solid line represents the evolution of probability over time when $\gamma=1/N$ ($\gamma=2/\sqrt{N}$) in the model with $N=1024$ and $k=20$.

In the demonstration of the optimal value for γ, we also provide the search results with different γs. In Figs. 2(c) and 2(d), we take the values of γ as $\gamma=\frac{1}{N}$ and $\gamma=\frac{2}{\sqrt{N}}$. The former (latter) value is smaller (larger) than the optimal value of γ. We can find that maximum search probabilities for these two cases are smaller than that in the search with $\gamma=\frac{2}{N}$.

3.2. The k_1 target vertices in red and $(k-k_1)$ target vertices in gray

When the target vertices are not all in red, the situation will be different. For the second case, it is assumed that there are k_1 target vertices in red and $(k-k_1)$ target vertices in gray. In this case, the vertices in the joined complete graph can be grounded into six categories in Eq. (6) as

$$
\begin{aligned}
&|a\rangle=\frac{1}{\sqrt{k_1}}\sum_{j\in\text{red}}|j\rangle,\quad |b\rangle=\frac{1}{\sqrt{\frac{N}{2}-k_1-1}}\sum_{j\in\text{blue}}|j\rangle,\\
&|c\rangle=|\text{yellow}\rangle,\quad |d\rangle=|\text{green}\rangle,\quad |e\rangle=\frac{1}{\sqrt{k-k_1}}\sum_{j\in\text{gray}}|j\rangle,\\
&|f\rangle=\frac{1}{\sqrt{\frac{N}{2}-k+k_1-1}}\sum_{j\in\text{white}}|j\rangle.
\end{aligned}
\tag{6}
$$

In Eq. (6), the "yellow" and "green" in "$|\rangle$" represent the vertices in yellow and green colors in Fig. 1, respectively. The vertex in yellow is the $\frac{N}{2}$th vertex in the graph, and the state is $|\text{yellow}\rangle=\left|\frac{N}{2}\right\rangle$. The vertex in green is the $\left(\frac{N}{2}+1\right)$th vertex in the graph, and the state is $|\text{green}\rangle=\left|\frac{N}{2}+1\right\rangle$. The Hamiltonian H can be expanded by these six bases as

$$
H=-\gamma\begin{pmatrix}
k_1-1+\frac{1}{\gamma} & \sqrt{k_1(\frac{N}{2}-k_1-1)} & \sqrt{k_1} & 0 & 0 & 0\\
\sqrt{k_1(\frac{N}{2}-k_1-1)} & \frac{N}{2}-k_1-2 & \sqrt{\frac{N}{2}-k_1-1} & 0 & 0 & 0\\
\sqrt{k_1} & \sqrt{\frac{N}{2}-k_1-1} & 0 & 1 & 0 & 0\\
0 & 0 & 1 & 0 & \sqrt{k-k_1} & \sqrt{\frac{N}{2}-k+k_1-1}\\
0 & 0 & 0 & \sqrt{k-k_1} & k-k_1-1+\frac{1}{\gamma} & \sqrt{(k-k_1)(\frac{N}{2}-k+k_1-1)}\\
0 & 0 & 0 & \sqrt{\frac{N}{2}-k+k_1-1} & \sqrt{(k-k_1)(\frac{N}{2}-k+k_1-1)} & \frac{N}{2}-k+k_1-2
\end{pmatrix}.
\tag{7}
$$

When the number of target vertices k is commonly far smaller than the number of total vertices N, we simplify H to

$$
H=-\gamma\begin{pmatrix}
\frac{1}{\gamma} & \sqrt{\frac{k_1N}{2}} & \sqrt{k_1} & 0 & 0 & 0\\
\sqrt{\frac{k_1N}{2}} & \frac{N}{2} & \sqrt{\frac{N}{2}} & 0 & 0 & 0\\
\sqrt{k_1} & \sqrt{\frac{N}{2}} & 0 & 1 & 0 & 0\\
0 & 0 & 1 & 0 & \sqrt{k-k_1} & \sqrt{\frac{N}{2}}\\
0 & 0 & 0 & \sqrt{k-k_1} & \frac{1}{\gamma} & \sqrt{\frac{N}{2}(k-k_1)}\\
0 & 0 & 0 & \sqrt{\frac{N}{2}} & \sqrt{\frac{N}{2}(k-k_1)} & \frac{N}{2}
\end{pmatrix}.
\tag{8}
$$

We also decompose this Hamiltonian as $H=H_0+H_1+H_2$ where the leading order matrix elements in H_0, H_1 and H_2 are N, $\sqrt{N}$ and 1, respectively. For the elements in H_2 are rather small when N is large, so we can neglect H_2 and provide the details of H_0 and H_1 as below:

$$
H_0=-\gamma\begin{pmatrix}
\frac{1}{\gamma} & 0 & 0 & 0 & 0 & 0\\
0 & \frac{N}{2} & 0 & 0 & 0 & 0\\
0 & 0 & 0 & 0 & 0 & 0\\
0 & 0 & 0 & 0 & 0 & 0\\
0 & 0 & 0 & 0 & \frac{1}{\gamma} & 0\\
0 & 0 & 0 & 0 & 0 & \frac{N}{2}
\end{pmatrix},\quad
H_1=-\gamma\begin{pmatrix}
0 & \sqrt{\frac{k_1N}{2}} & 0 & 0 & 0 & 0\\
\sqrt{\frac{k_1N}{2}} & 0 & \sqrt{\frac{N}{2}} & 0 & 0 & 0\\
0 & \sqrt{\frac{N}{2}} & 0 & 0 & 0 & 0\\
0 & 0 & 0 & 0 & 0 & \sqrt{\frac{N}{2}}\\
0 & 0 & 0 & 0 & 0 & \sqrt{\frac{N}{2}(k-k_1)}\\
0 & 0 & 0 & \sqrt{\frac{N}{2}} & \sqrt{\frac{N}{2}(k-k_1)} & 0
\end{pmatrix}.
\tag{9}
$$

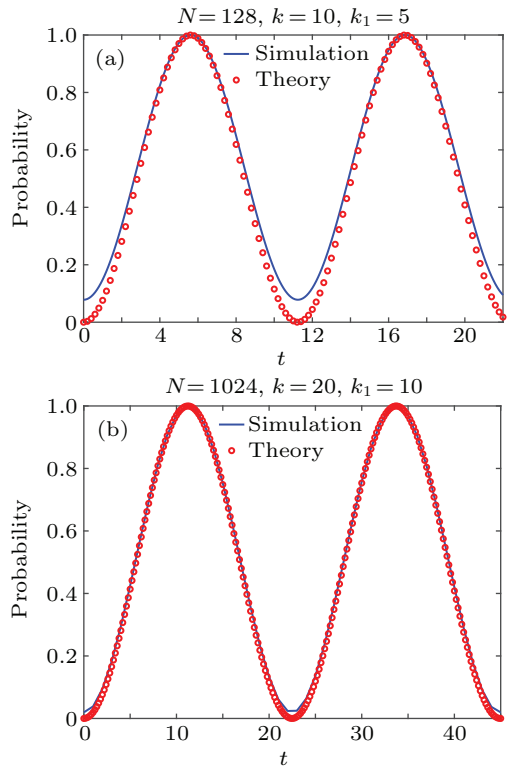


Fig. 3. The success search probability of target vertices in the joined complete graph. In this case, k_1 target vertices in red and $(k-k_1)$ target vertices in gray. The total number of vertices in (a) and (b) are 128 and 1024, respectively. The number of target vertices in red (gray) in (a) and (b) are 5 (5) and 10 (10), respectively. The value of $\gamma = 2/N$. In two panels, the red dots are the theoretic derivation of probability above. Blue solid lines represent the numerical results obtained by quantum walk evolution under N dimensional Hilbert space.

For the Hamiltonian H_0, it is assumed that $\frac{1}{\gamma} = \frac{N}{2}$ which makes the corresponding states $|a\rangle$, $|b\rangle$, $|e\rangle$ and $|f\rangle$ become degenerated states. So we set $\gamma = \frac{2}{N}$. The terms in $H_0 + H_1$ which describe the connections between $|a\rangle$, $|b\rangle$, $|e\rangle$ and $|f\rangle$ can be re-expressed in one matrix spanned by these four bases. The corresponding eigenstates of such matrix are $|\varphi_1\rangle = \frac{1}{\sqrt{2}}(|e\rangle + |f\rangle)|\varphi_2\rangle = \frac{1}{\sqrt{2}}(|a\rangle + |b\rangle)$, $|\varphi_3\rangle = \frac{1}{\sqrt{2}}(-|a\rangle + |b\rangle)$ and $|\varphi_4\rangle = \frac{1}{\sqrt{2}}(-|e\rangle + |f\rangle)$. The corresponding eigenvalues are $E_1 = -\sqrt{\frac{2(k-k_1)}{N}} - 1$, $E_2 = -\sqrt{\frac{2k_1}{N}} - 1$, $E_3 = \sqrt{\frac{2k_1}{N}} - 1$ and $E_4 = \sqrt{\frac{2(k-k_1)}{N}} - 1$, respectively. The initial state $|s\rangle \approx \frac{1}{\sqrt{2}}(|b\rangle + |f\rangle) = \frac{1}{2}(|\varphi_1\rangle + |\varphi_2\rangle + |\varphi_3\rangle + |\varphi_4\rangle)$ when N is large. In this case, the target vertices are represented by $|a+e\rangle = \frac{1}{\sqrt{2}}|a\rangle + \frac{1}{\sqrt{2}}|e\rangle$, so the success amplitude of finding target state is $\langle a+e|\varphi(t)\rangle = \langle a+e|\, \mathrm{e}^{-\mathrm{i}(H_0+H_1)t}\,|s\rangle = \frac{1}{2}\mathrm{e}^{\mathrm{i}t}\mathrm{i}(\sin\sqrt{\frac{2(k-k_1)}{N}}t + \sin\sqrt{\frac{2k_1}{N}}t)$. The success probability is $P = \left|\frac{1}{2}\mathrm{e}^{\mathrm{i}t}\mathrm{i}(\sin\sqrt{\frac{2(k-k_1)}{N}}t + \sin\sqrt{\frac{2k_1}{N}}t)\right|^2$.

In Fig. 3, we provide the numerical (blue lines) and theoretic (red dots) results in the search of red and gray vertices. As reflected from these two panels, the numerical and theoretical results coincide with each other well. For case B with the target vertices locating at two complete graphs, the maximum searching probability reaches 1 with the optimal jumping rate, which means the successful search has been realized. Compared with Figs. 3(a) and 3(b), we can find that the difference between the numerical and theoretical results becomes smaller when the number of vertices is larger. When the total number of vertices is $N = 128\,(1024)$, the maximum success probability in finding these vertices is achieved at the first time at $t = 5.6\,(11.2)$. So this time is proportional to $\sqrt{N}$.

3.3. The $(k-1)$ target vertices in red and one target vertex in yellow

In this case, the situations are different from above. One of the target vertices locates at the position in the graph possessing different connectivity with the other target vertices. Here we assume there are $(k-1)$ target vertices in red and the remaining one target vertex in yellow. So the vertices in gray and in white can be viewed as one type of vertices having the same properties. We can group the total vertices into five categories as follows:

$$\begin{aligned} &|a\rangle = \frac{1}{\sqrt{k-1}}\sum_{j\in\text{red}}|j\rangle, \quad |b\rangle = \frac{1}{\sqrt{\frac{N}{2}-k}}\sum_{j\in\text{blue}}|j\rangle, \\ &|c\rangle = |\text{yellow}\rangle, \quad |d\rangle = |\text{green}\rangle, \\ &|e\rangle = \frac{1}{\sqrt{\frac{N}{2}-1}}\sum_{\substack{j\in\text{white}\\ \&\text{gray}}}|j\rangle. \end{aligned} \tag{10}$$

In Eq. (10), the "yellow" and "green" in "$|\,\rangle$" represent the vertices in yellow and green colors in Fig. 1, respectively. The vertex in yellow is the $\frac{N}{2}$th vertex in the graph, and the state is $|\text{yellow}\rangle = |\frac{N}{2}\rangle$. The vertex in green is the $(\frac{N}{2}+1)$th vertex in the graph, and the state is $|\text{green}\rangle = |\frac{N}{2}+1\rangle$. The searching Hamiltonian can be obtained with these five bases as

$$H = -\gamma\begin{pmatrix} k-2+\frac{1}{\gamma} & \sqrt{(k-1)(\frac{N}{2}-k)} & \sqrt{k-1} & 0 & 0 \\ \sqrt{(k-1)(\frac{N}{2}-k)} & \frac{N}{2}-k-1 & \sqrt{\frac{N}{2}-k} & 0 & 0 \\ \sqrt{k-1} & \sqrt{\frac{N}{2}-k} & \frac{1}{\gamma} & 1 & 0 \\ 0 & 0 & 1 & 0 & \sqrt{\frac{N}{2}-1} \\ 0 & 0 & 0 & \sqrt{\frac{N}{2}-1} & \frac{N}{2}-2 \end{pmatrix}. \tag{11}$$

When the number of target vertices k is commonly far smaller than the number of total vertices N, we simplify H to

$$H=-\gamma\begin{pmatrix}\frac{1}{\gamma} & \sqrt{(k-1)\frac{N}{2}} & \sqrt{k-1} & 0 & 0\\ \sqrt{(k-1)\frac{N}{2}} & \frac{N}{2} & \sqrt{\frac{N}{2}} & 0 & 0\\ \sqrt{k-1} & \sqrt{\frac{N}{2}} & \frac{1}{\gamma} & 1 & 0\\ 0 & 0 & 1 & 0 & \sqrt{\frac{N}{2}}\\ 0 & 0 & 0 & \sqrt{\frac{N}{2}} & \frac{N}{2}\end{pmatrix}. \quad (12)$$

We also decompose this Hamiltonian as $H=H_0+H_1+H_2$ where the leading order matrix elements in H_0, H_1 and H_2 are N, $\sqrt{N}$ and 1, respectively. For the elements in H_2 are rather small when N is large, so we can neglect H_2 and provide the details of H_0 and H_1 as below:

$$H_0=-\gamma\begin{pmatrix}\frac{1}{\gamma} & 0 & 0 & 0 & 0\\ 0 & \frac{N}{2} & 0 & 0 & 0\\ 0 & 0 & \frac{1}{\gamma} & 0 & 0\\ 0 & 0 & 0 & 0 & 0\\ 0 & 0 & 0 & 0 & \frac{N}{2}\end{pmatrix},$$

$$H_1=-\gamma\begin{pmatrix}0 & \sqrt{\frac{N}{2}(k-1)} & 0 & 0 & 0\\ \sqrt{\frac{N}{2}(k-1)} & 0 & \sqrt{\frac{N}{2}} & 0 & 0\\ 0 & \sqrt{\frac{N}{2}} & 0 & 0 & 0\\ 0 & 0 & 0 & 0 & \sqrt{\frac{N}{2}}\\ 0 & 0 & 0 & \sqrt{\frac{N}{2}} & 0\end{pmatrix}. \quad (13)$$

For the Hamiltonian H_0, it is assumed that $\frac{1}{\gamma}=\frac{N}{2}$ which makes the corresponding states $|a\rangle$, $|b\rangle$, $|c\rangle$ and $|e\rangle$ become degenerated states. So we set $\gamma=\frac{2}{N}$. The terms in H_0+H_1 which describe the connections between $|a\rangle$, $|b\rangle$, $|c\rangle$ and $|e\rangle$ can be re-expressed in one matrix spanned by these four bases. The corresponding eigenstates of such matrix are $|\varphi_1\rangle=\frac{1}{\sqrt{2k}}(\sqrt{k-1}\,|a\rangle+\sqrt{k}\,|b\rangle+|c\rangle)$, $|\varphi_2\rangle=|e\rangle$, $|\varphi_3\rangle=\sqrt{\frac{k-1}{k}}(-\frac{1}{\sqrt{k-1}}\,|a\rangle+|c\rangle)$ and $|\varphi_4\rangle=\frac{1}{\sqrt{2k}}(\sqrt{k-1}\,|a\rangle-\sqrt{k}\,|b\rangle+|c\rangle)$. The corresponding eigenvalues are $E_1=-1-\sqrt{\frac{2k}{N}}$, $E_2=-1$, $E_3=-1$ and $E_4=-1+\sqrt{\frac{2k}{N}}$, respectively. The initial state $|s\rangle\approx\frac{1}{\sqrt{2}}(|b\rangle+|e\rangle)=\frac{1}{2}(|\varphi_1\rangle-|\varphi_4\rangle)+\frac{1}{\sqrt{2}}|\varphi_2\rangle$ when N is large. In this case, the target vertices are represented by $|a+c\rangle=\frac{1}{\sqrt{2}}|a\rangle+\frac{1}{\sqrt{2}}|c\rangle$, so the success amplitude of finding target state is $\langle a+c|\varphi(t)\rangle=\langle a+c|\,\mathrm{e}^{-\mathrm{i}(H_0+H_1)t}\,|s\rangle=\frac{1}{2\sqrt{k}}(\sqrt{k-1}+1)\,\mathrm{e}^{\mathrm{i}t}\mathrm{i}\sin\sqrt{\frac{2k}{N}}t$. The success probability is $P=|\langle a+c|\varphi(t)\rangle|^2=\frac{1}{4k}(\sqrt{k-1}+1)^2\sin^2\sqrt{\frac{2k}{N}}t$. The time to achieve the maximum searching probability is $t=\frac{\pi}{2}\sqrt{\frac{N}{2k}}$.

In Fig. 4, we provide the numerical (blue lines) and theoretical (red dots) results. Here, the target vertices are composed by the red vertices and the yellow vertex. The total number of target vertices are both 4 in these two scenarios. As reflected from these two panels, the numerical and theoretical results agree with each other well. For case C with the target vertices locating at the left complete graph, the maximum searching probability reaches 1/2 with the optimal jumping rate, which means the successful search has been realized. Compared with Figs. 4(a) and 4(b), we can find that the difference between the numerical and theoretical results becomes smaller when the number of vertices is larger. When the total number of vertices is $N=128\,(1024)$, the maximum success probability in finding these vertices is achieved at the first time at $t=6.28\,(17.77)$.

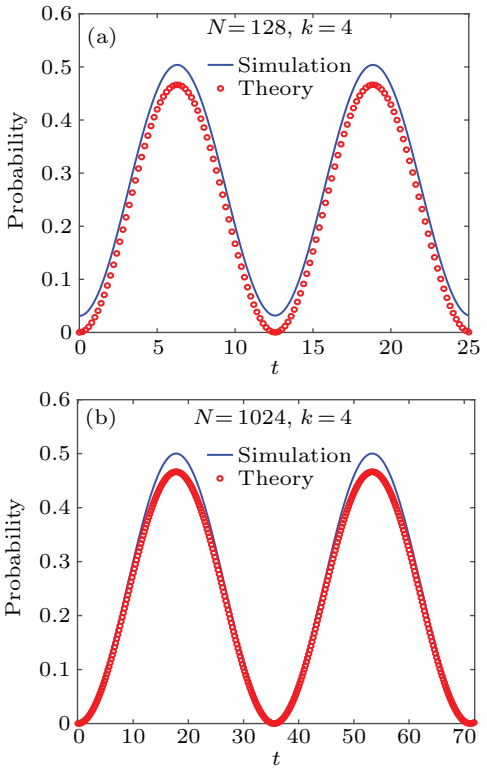


Fig. 4. The success search probability of target vertices in the joined complete graph. In this case, $(k-1)$ target vertices in red and the remaining target vertex in yellow. The total number of vertices in (a) and (b) are 128 and 1024, respectively. The number of target vertices in red in (a) and (b) are both $k-1=3$. The value of $\gamma=2/N$. In two panels, red dots are theoretic derivations of probability above. Blue solid lines represent numerical results obtained by quantum walk evolution under N dimensional Hilbert space.

3.4. The (k_1-1) target vertices in red, one in yellow and $(k-k_1)$ target vertices in gray

Here, the target vertices are distributed into two complete graphs and one of them locates at the position with different connectivity. There are (k_1-1) target vertices in red, one target vertex in yellow, and $(k-k_1)$ target vertices in gray. So we can group these vertices into six categories

$$|a\rangle=\frac{1}{\sqrt{k_1-1}}\sum_{j\in\mathrm{red}}|j\rangle,\quad |b\rangle=\frac{1}{\sqrt{\frac{N}{2}-k_1}}\sum_{j\in\mathrm{blue}}|j\rangle,$$

$$|c\rangle=|\mathrm{yellow}\rangle,\quad |d\rangle=|\mathrm{green}\rangle,\quad |e\rangle=\frac{1}{\sqrt{k-k_1}}\sum_{j\in\mathrm{gray}}|j\rangle,$$

$$|f\rangle = \frac{1}{\sqrt{\frac{N}{2}-k+k_1-1}} \sum_{j\in\text{white}} |j\rangle. \tag{14}$$

In Eq. (14), the "yellow" and "green" in "$|\rangle$" represent the vertices in yellow and green colors in Fig. 1, respectively. The vertex in yellow is the $\frac{N}{2}$th vertex in the graph, and the state is $|\text{yellow}\rangle = \left|\frac{N}{2}\right\rangle$. The vertex in green is the $\left(\frac{N}{2}+1\right)$th vertex in the graph, and the state is $|\text{green}\rangle = \left|\frac{N}{2}+1\right\rangle$. The searching Hamiltonian can be obtained with these six bases as

$$H = -\gamma \begin{pmatrix} k_1-2+\frac{1}{\gamma} & \sqrt{(\frac{N}{2}-k_1)(k_1-1)} & \sqrt{k_1-1} & 0 & 0 & 0 \\ \sqrt{(\frac{N}{2}-k_1)(k_1-1)} & \frac{N}{2}-k_1-1 & \sqrt{\frac{N}{2}-k_1} & 0 & 0 & 0 \\ \sqrt{k_1-1} & \sqrt{\frac{N}{2}-k_1} & \frac{1}{\gamma} & 1 & 0 & 0 \\ 0 & 0 & 1 & 0 & \sqrt{k-k_1} & \sqrt{\frac{N}{2}-k+k_1-1} \\ 0 & 0 & 0 & \sqrt{k-k_1} & k-k_1-1+\frac{1}{\gamma} & \sqrt{(\frac{N}{2}-k+k_1-1)(k-k_1)} \\ 0 & 0 & 0 & \sqrt{\frac{N}{2}-k+k_1-1} & \sqrt{(\frac{N}{2}-k+k_1-1)(k-k_1)} & \frac{N}{2}-k+k_1-2 \end{pmatrix}. \tag{15}$$

When the number of target vertices k is commonly far smaller than the number of total vertices N, we simplify H to

$$H = -\gamma \begin{pmatrix} \frac{1}{\gamma} & \sqrt{\frac{N}{2}(k_1-1)} & \sqrt{k_1-1} & 0 & 0 & 0 \\ \sqrt{\frac{N}{2}(k_1-1)} & \frac{N}{2} & \sqrt{\frac{N}{2}} & 0 & 0 & 0 \\ \sqrt{k_1-1} & \sqrt{\frac{N}{2}} & \frac{1}{\gamma} & 1 & 0 & 0 \\ 0 & 0 & 1 & 0 & \sqrt{k-k_1} & \sqrt{\frac{N}{2}} \\ 0 & 0 & 0 & \sqrt{k-k_1} & \frac{1}{\gamma} & \sqrt{\frac{N}{2}(k-k_1)} \\ 0 & 0 & 0 & \sqrt{\frac{N}{2}} & \sqrt{\frac{N}{2}(k-k_1)} & \frac{N}{2} \end{pmatrix}. \tag{16}$$

We also decompose this Hamiltonian as $H = H_0 + H_1 + H_2$ where the leading order matrix elements in H_0, H_1 and H_2 are N, $\sqrt{N}$ and 1, respectively. For the elements in H_2 are rather small when N is large, so we can neglect H_2 and provide the details of H_0 and H_1 in as below:

$$H_0 = -\gamma \begin{pmatrix} \frac{1}{\gamma} & 0 & 0 & 0 & 0 & 0 \\ 0 & \frac{N}{2} & 0 & 0 & 0 & 0 \\ 0 & 0 & \frac{1}{\gamma} & 0 & 0 & 0 \\ 0 & 0 & 0 & 0 & 0 & 0 \\ 0 & 0 & 0 & 0 & \frac{1}{\gamma} & 0 \\ 0 & 0 & 0 & 0 & 0 & \frac{N}{2} \end{pmatrix}, \quad H_1 = -\gamma \begin{pmatrix} 0 & \sqrt{\frac{N}{2}(k_1-1)} & 0 & 0 & 0 & 0 \\ \sqrt{\frac{N}{2}(k_1-1)} & 0 & \sqrt{\frac{N}{2}} & 0 & 0 & 0 \\ 0 & \sqrt{\frac{N}{2}} & 0 & 0 & 0 & 0 \\ 0 & 0 & 0 & 0 & 0 & \sqrt{\frac{N}{2}} \\ 0 & 0 & 0 & 0 & 0 & \sqrt{\frac{N}{2}(k-k_1)} \\ 0 & 0 & 0 & \sqrt{\frac{N}{2}} & \sqrt{\frac{N}{2}(k-k_1)} & 0 \end{pmatrix}. \tag{17}$$

For the Hamiltonian H_0, it is assumed that $\frac{1}{\gamma} = \frac{N}{2}$ which makes the corresponding states $|a\rangle$, $|b\rangle$, $|c\rangle$, $|e\rangle$ and $|f\rangle$ become degenerated states. So we set $\gamma = \frac{2}{N}$. The terms in $H_0 + H_1$ which describe the connections between $|a\rangle$, $|b\rangle$, $|c\rangle$, $|e\rangle$ and $|f\rangle$ can be re-expressed in one matrix spanned by these five bases. The corresponding eigenstates of such matrix are $|\varphi_1\rangle = \frac{1}{\sqrt{2}}(|e\rangle + |f\rangle)$, $|\varphi_2\rangle = \frac{1}{\sqrt{2k_1}}(\sqrt{k_1-1}\,|a\rangle + \sqrt{k_1}\,|b\rangle + |c\rangle)$, $|\varphi_3\rangle = \frac{1}{\sqrt{2}}(-|a\rangle + |c\rangle)$, $|\varphi_4\rangle = \frac{1}{\sqrt{2k_1}}(\sqrt{k_1-1}\,|a\rangle - \sqrt{k_1}\,|b\rangle + |c\rangle)$ and $|\varphi_5\rangle = \frac{1}{\sqrt{2}}(-|e\rangle + |f\rangle)$. The corresponding eigenvalues are $E_1 = -1 - \sqrt{\frac{2}{N}(k-k_1)}$, $E_2 = -1 - \sqrt{\frac{2k_1}{N}}$, $E_3 = -1$, $E_4 = -1 + \sqrt{\frac{2k_1}{N}}$ and $E_5 = -1 + \sqrt{\frac{2}{N}(k-k_1)}$, respectively. The initial state $|s\rangle \approx \frac{1}{\sqrt{2}}(|b\rangle + |f\rangle) = \frac{1}{2}(|\varphi_2\rangle - |\varphi_4\rangle + |\varphi_1\rangle + |\varphi_5\rangle)$ when N is large. In this case, the target vertices are represented by $|a+c+e\rangle = \frac{1}{\sqrt{3}}|a\rangle + \frac{1}{\sqrt{3}}|c\rangle + \frac{1}{\sqrt{3}}|e\rangle$, so the success amplitude of finding target state is $\langle a+c+e\,|\varphi(t)\rangle = \langle a+c+e|\,\mathrm{e}^{-\mathrm{i}(H_0+H_1)t}\,|s\rangle = \frac{1}{\sqrt{6k_1}}(\sqrt{k_1-1}+1)\,\mathrm{e}^{\mathrm{i}t}\,\mathrm{i}\sin\sqrt{\frac{2k_1}{N}}t + \frac{1}{\sqrt{6}}\,\mathrm{e}^{\mathrm{i}t}\,\mathrm{i}\sin\sqrt{\frac{2(k-k_1)}{N}}t$. The success probability is

$$P = \left| \frac{1}{\sqrt{6k_1}}(\sqrt{k_1-1}+1)\,\mathrm{e}^{\mathrm{i}t}\,\mathrm{i}\sin\sqrt{\frac{2k_1}{N}}t + \frac{1}{\sqrt{6}}\,\mathrm{e}^{\mathrm{i}t}\,\mathrm{i}\sin\sqrt{\frac{2(k-k_1)}{N}}t \right|^2.$$

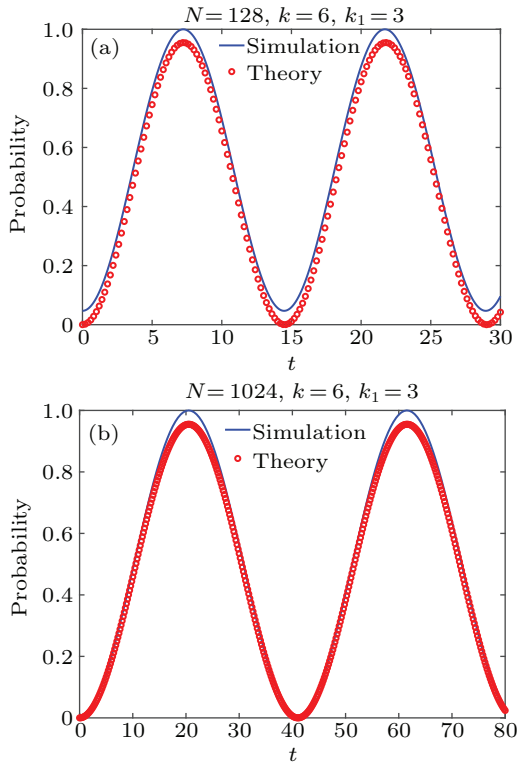


Fig. 5. The success search probability of target vertices in the joined complete graph. In this case, (k_1-1) target vertices in red, one target vertex in yellow and $(k-k_1)$ target vertices in gray. The total number of vertices in (a) and (b) are 128 and 1024, respectively. The number of target vertices in red (gray) in (a) and (b) are both 2 (3). The value of $\gamma = 2/N$. In two panels, the red dots are the theoretic derivation of probability above. Blue solid lines represent the numerical results obtained by quantum walk evolution under N dimensional Hilbert space.

In Fig. 5, we provide the numerical (blue lines) and theoretical (red dots) results. In this case, the target vertices are (k_1-1) in red, one in yellow and $(k-k_1)$ in gray. As reflected from these two panels, the numerical and theoretical results coincide with each other well. For case D with the target vertices locating at two complete graphs, the maximum searching probability reaches 1 with the optimal jumping rate, which means the successful search has been realized. Compared with Figs. 5(a) and 5(b), we can find that the difference between the numerical and theoretic results becomes smaller when the number of vertices is larger. When the total number of vertices is $N = 128\,(1024)$, the maximum success probability in finding these vertices is achieved at the first time at $t = 7.2\,(20.5)$. So this time is proportional to $\sqrt{N}$.

3.5. The (k_1-1) target vertices in red, one in yellow, one in green, and the remaining $(k-k_1-1)$ in gray

Here, we consider another case that the target vertices locate at each complete graph. There are (k_1-1) target vertices in red, one in yellow, one in green, and $(k-k_1-1)$ target vertices in gray. All of the vertices can be grouped into six categories as

$$|a\rangle = \frac{1}{\sqrt{k_1-1}}\sum_{j\in\text{red}}|j\rangle,\quad |b\rangle = \frac{1}{\sqrt{\frac{N}{2}-k_1}}\sum_{j\in\text{blue}}|j\rangle,$$
$$|c\rangle = |\text{yellow}\rangle,\quad |d\rangle = |\text{green}\rangle,\quad |e\rangle = \frac{1}{\sqrt{k-k_1-1}}\sum_{j\in\text{gray}}|j\rangle,$$
$$|f\rangle = \frac{1}{\sqrt{\frac{N}{2}-k+k_1}}\sum_{j\in\text{white}}|j\rangle. \tag{18}$$

In Eq. (18), the "yellow" and "green" in "$|\rangle$" represent the vertices in yellow and green colors in Fig. 1, respectively. The vertex in yellow is the $\frac{N}{2}$th vertex in the graph, and the state is $|\text{yellow}\rangle = \left|\frac{N}{2}\right\rangle$. The vertex in green is the $\left(\frac{N}{2}+1\right)$th vertex in the graph, and the state is $|\text{green}\rangle = \left|\frac{N}{2}+1\right\rangle$. The searching Hamiltonian can be obtained with these six bases as

$$H = -\gamma\begin{pmatrix} k_1-2+\frac{1}{\gamma} & \sqrt{(k_1-1)(\frac{N}{2}-k_1)} & \sqrt{k_1-1} & 0 & 0 & 0 \\ \sqrt{(k_1-1)(\frac{N}{2}-k_1)} & \frac{N}{2}-k_1-1 & \sqrt{\frac{N}{2}-k_1} & 0 & 0 & 0 \\ \sqrt{k_1-1} & \sqrt{\frac{N}{2}-k_1} & \frac{1}{\gamma} & 1 & 0 & 0 \\ 0 & 0 & 1 & \frac{1}{\gamma} & \sqrt{k-k_1-1} & \sqrt{\frac{N}{2}-k+k_1} \\ 0 & 0 & 0 & \sqrt{k-k_1-1} & k-k_1-2+\frac{1}{\gamma} & \sqrt{(k-k_1-1)(\frac{N}{2}-k+k_1)} \\ 0 & 0 & 0 & \sqrt{\frac{N}{2}-k+k_1} & \sqrt{(k-k_1-1)(\frac{N}{2}-k+k_1)} & \frac{N}{2}-k+k_1-1 \end{pmatrix}. \tag{19}$$

When the number of target vertices k is commonly far smaller than the number of total vertices N, we simplify H to

$$H = -\gamma\begin{pmatrix} \frac{1}{\gamma} & \sqrt{(k_1-1)\frac{N}{2}} & \sqrt{k_1-1} & 0 & 0 & 0 \\ \sqrt{(k_1-1)\frac{N}{2}} & \frac{N}{2} & \sqrt{\frac{N}{2}} & 0 & 0 & 0 \\ \sqrt{k_1-1} & \sqrt{\frac{N}{2}} & \frac{1}{\gamma} & 1 & 0 & 0 \\ 0 & 0 & 1 & \frac{1}{\gamma} & \sqrt{k-k_1-1} & \sqrt{\frac{N}{2}} \\ 0 & 0 & 0 & \sqrt{k-k_1-1} & \frac{1}{\gamma} & \sqrt{(k-k_1-1)\frac{N}{2}} \\ 0 & 0 & 0 & \sqrt{\frac{N}{2}} & \sqrt{(k-k_1-1)\frac{N}{2}} & \frac{N}{2} \end{pmatrix}. \tag{20}$$

We also decompose this Hamiltonian as $H = H_0 + H_1 + H_2$ where the leading order matrix elements in H_0, H_1 and H_2 are N, $\sqrt{N}$ and 1, respectively. For the elements in H_2 are rather small when N is large, so we can neglect H_2 and provide the details of H_0 and H_1 as below:

$$H_0 = -\gamma \begin{pmatrix} \frac{1}{\gamma} & 0 & 0 & 0 & 0 & 0 \\ 0 & \frac{N}{2} & 0 & 0 & 0 & 0 \\ 0 & 0 & \frac{1}{\gamma} & 0 & 0 & 0 \\ 0 & 0 & 0 & \frac{1}{\gamma} & 0 & 0 \\ 0 & 0 & 0 & 0 & \frac{1}{\gamma} & 0 \\ 0 & 0 & 0 & 0 & 0 & \frac{N}{2} \end{pmatrix}, \quad H_1 = -\gamma \begin{pmatrix} 0 & \sqrt{(k_1-1)\frac{N}{2}} & 0 & 0 & 0 & 0 \\ \sqrt{(k_1-1)\frac{N}{2}} & 0 & \sqrt{\frac{N}{2}} & 0 & 0 & 0 \\ 0 & \sqrt{\frac{N}{2}} & 0 & 0 & 0 & 0 \\ 0 & 0 & 0 & 0 & 0 & \sqrt{\frac{N}{2}} \\ 0 & 0 & 0 & 0 & 0 & \sqrt{(k-k_1-1)\frac{N}{2}} \\ 0 & 0 & 0 & \sqrt{\frac{N}{2}} & \sqrt{(k-k_1-1)\frac{N}{2}} & 0 \end{pmatrix}. \quad (21)$$

For the Hamiltonian H_0, it is assumed that $\frac{1}{\gamma} = \frac{N}{2}$ which makes the corresponding states $|a\rangle$, $|b\rangle$, $|c\rangle$, $|d\rangle$, $|e\rangle$ and $|f\rangle$ become degenerated states. So we set $\gamma = \frac{2}{N}$. The terms in $H_0 + H_1$ which describe the connections between $|a\rangle$, $|b\rangle$, $|c\rangle$, $|d\rangle$, $|e\rangle$ and $|f\rangle$ can be re-expressed in one matrix spanned by these six bases. The corresponding eigenstates of such matrix are $|\varphi_1\rangle = \frac{1}{\sqrt{2}}(\frac{1}{\sqrt{k-k_1}}|d\rangle + \sqrt{1-\frac{1}{k-k_1}}|e\rangle + |f\rangle)$, $|\varphi_2\rangle = \frac{1}{\sqrt{2k_1}}(\sqrt{k_1-1}|a\rangle + \sqrt{k_1}|b\rangle + |c\rangle)$, $|\varphi_3\rangle = \sqrt{\frac{k_1-1}{k_1}}(-\frac{1}{\sqrt{k_1-1}}|a\rangle + |c\rangle)$, $|\varphi_4\rangle = \frac{1}{\sqrt{k-k_1}}(-\sqrt{k-k_1-1}|d\rangle + |e\rangle)$, $|\varphi_5\rangle = \frac{1}{\sqrt{2k_1}}(\sqrt{k_1-1}|a\rangle - \sqrt{k_1}|b\rangle + |c\rangle)$ and $|\varphi_6\rangle = \frac{1}{\sqrt{2}}(-\frac{1}{\sqrt{k-k_1}}|d\rangle - \sqrt{1-\frac{1}{k-k_1}}|e\rangle + |f\rangle)$. The corresponding eigenvalues are $E_1 = -1-\sqrt{\frac{2(k-k_1)}{N}}$, $E_2 = -1-\sqrt{\frac{2k_1}{N}}$, $E_3 = -1$, $E_4 = -1$, $E_5 = -1+\sqrt{\frac{2k_1}{N}}$ and $E_6 = -1+\sqrt{\frac{2(k-k_1)}{N}}$, respectively. The initial state $|s\rangle \approx \frac{1}{\sqrt{2}}(|b\rangle + |f\rangle) = \frac{1}{2}(|\varphi_2\rangle - |\varphi_5\rangle + |\varphi_1\rangle + |\varphi_6\rangle)$ when N is large. In this case, the target vertices are represented by $|a+c+d+e\rangle = \frac{1}{2}|a\rangle + \frac{1}{2}|c\rangle + \frac{1}{2}|d\rangle + \frac{1}{2}|e\rangle$, so the success amplitude of finding target state is

$$\begin{aligned} &\langle a+c+d+e|\varphi(t)\rangle \\ &= \frac{1}{2\sqrt{2k_1}}(\sqrt{k_1-1}+1)\,\mathrm{e}^{\mathrm{i}t}\,\mathrm{i}\sin\sqrt{\frac{2k_1}{N}}t \\ &\quad + \frac{1}{2\sqrt{2}}\left(\frac{1}{\sqrt{k-k_1}} + \sqrt{1-\frac{1}{k-k_1}}\right)\mathrm{e}^{\mathrm{i}t}\,\mathrm{i}\sin\sqrt{\frac{2(k-k_1)}{N}}t. \end{aligned}$$

The success probability is

$$\begin{aligned} P = &\left|\frac{1}{2\sqrt{2k_1}}(\sqrt{k_1-1}+1)\,\mathrm{e}^{\mathrm{i}t}\,\mathrm{i}\sin\sqrt{\frac{2k_1}{N}}t\right. \\ &\left. + \frac{1}{2\sqrt{2}}\left(\frac{1}{\sqrt{k-k_1}} + \sqrt{1-\frac{1}{k-k_1}}\right)\mathrm{e}^{\mathrm{i}t}\,\mathrm{i}\sin\sqrt{\frac{2(k-k_1)}{N}}t\right|^2. \end{aligned}$$

In Fig. 6, we provide the numerical (blue lines) and theoretic (red dots) results. In this case, the target vertices are (k_1-1) in red, one in yellow, one in green and $(k-k_1-1)$ in gray. As revealed from these two panels, the numerical and theoretic results coincide with each other well. For case E with the target vertices locating at two complete graphs, the maximum searching probability reaches 1 with the optimal jumping rate, which means the successful search has been realized. Compared with Figs. 6(a) and 6(b), we can find that the difference between the numerical and theoretical results becomes smaller at the beginning of the evolution when the number of vertices is larger. When the total number of vertices is $N = 128\,(1024)$, the maximum success probability in finding these vertices is achieved at the first time at $t = 7.2\,(17.8)$.

In the following, we provide a table to summarize the results of the above derivation.

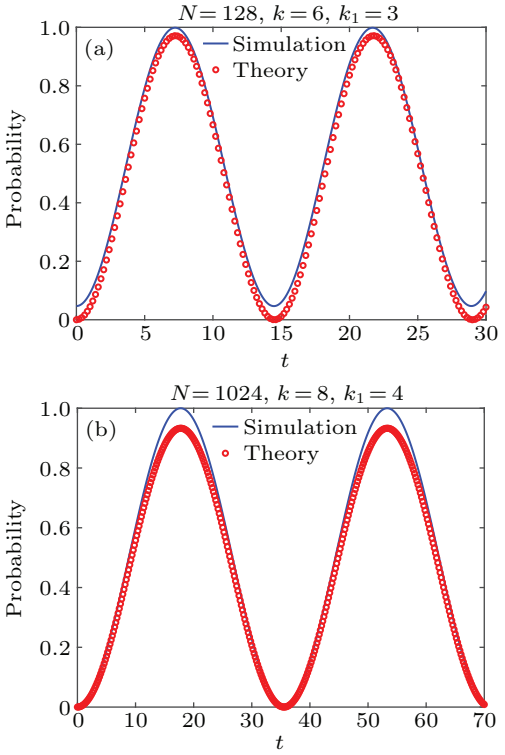
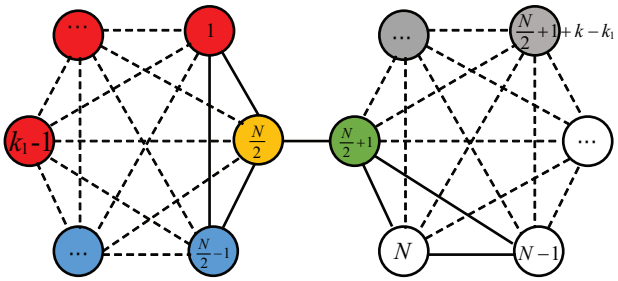


Fig. 6. The success search probability of target vertices in the joined complete graph. In this case, (k_1-1) target vertices in red, one target vertex in yellow, one in green and $(k-k_1-1)$ target vertices in gray. The total number of vertices in (a) and (b) are 128 and 1024, respectively. The number of target vertices in red (gray) in (a) and (b) are 2 and 3 (2 and 3), respectively. The value of $\gamma = 2/N$. In two panels, the red dots are the theoretic derivation of probability above. Blue solid lines represent the numerical results obtained by quantum walk evolution under N dimensional Hilbert space.

Table 1. The quantum search on the joined complete graph. The colors for the target vertices are shown in cases A–E.

Model			
Cases	Maximum success probability	Runtime	N, k and k_1 (example)
Case A: red	$p=\frac{1}{2}\sin^2\sqrt{\frac{2k}{N}}t$	$t\propto\sqrt{N}$	$N=128$, $k=5$, $t=5.62$; $N=1024$, $k=20$, $t=7.95$
Case B: red and gray	$P=\left\|\frac{1}{2}\mathrm{e}^{\mathrm{i}t}\mathrm{i}\left(\sin\sqrt{\frac{2(k-k_1)}{N}}t+\sin\sqrt{\frac{2k_1}{N}}t\right)\right\|^2$		$N=128$, $k=10$, $k_1=5$, $t=5.6$; $N=1024$, $k=20$, $k_1=10$, $t=11.2$
Case C: red and yellow	$p=\left[\frac{1}{2\sqrt{k}}(\sqrt{k-1}+1)\right]^2$		$N=128$, $k=4$, $t=6.28$; $N=1024$, $k=4$, $t=17.77$
Case D: red, yellow and gray	$p=\left\|\frac{1}{\sqrt{6}}\left[\frac{1}{\sqrt{k_1}}(\sqrt{k_1-1}+1)\sin\sqrt{\frac{2k_1}{N}}t+\sin\sqrt{\frac{2(k-k_1)}{N}}t\right]\right\|^2$		$N=128$, $k=6$, $k_1=3$, $t=7.2$; $N=1024$, $k=6$, $k_1=3$, $t=20.5$
Case E: red, yellow, green and gray	$p=\left\|\frac{1}{2\sqrt{2}}\left[\frac{1}{\sqrt{k_1}}(\sqrt{k_1-1}+1)\sin\sqrt{\frac{2k_1}{N}}t+\left(\frac{1}{\sqrt{k-k_1}}+\sqrt{1-\frac{1}{k-k_1}}\right)\sin\sqrt{\frac{2(k-k_1)}{N}}t\right]\right\|^2$		$N=128$, $k=6$, $k_1=3$, $t=7.2$; $N=1024$, $k=8$, $k_1=4$, $t=17.8$

4. Conclusion

In our work, we study the quantum search in one low-connectivity graph, which is the joined complete graph. The target vertices in the search is not limited one, and the possibilities of their distributions in the graph are analyzed in detail. Following the method presented in Ref. [30], we find that, when the target vertices distribute in the graph differently, the success probability of finding these vertices and the corresponding required time are also different. Whatever the positions of the target vertices, these vertices can be found in the time $O\left(\sqrt{N}\right)$ with the optimal jumping rate. Our theoretical results verify that for such low-connectivity graph, the search of many vertices possessing quantum advantage appear. Moreover, our results might be applicable for other graphs. It will provide strong evidence for practical quantum search algorithms.

Acknowledgements

Project supported by the National Key R&D Program of China (Grant No. 2017YFA0303800) and the National Natural Science Foundation of China (Grant Nos. 91850205 and 11974046).

References

[1] Grover L K 1998 *Phys. Rev. Lett.* **80** 4329
[2] Long G L 2001 *Phys. Rev. A* **64** 022307
[3] Long G L and Xiao L 2003 *J. Chem. Phys.* **119** 8473
[4] Aharonov D, Ambainis A, Kempe J and Vazirani U 2001 *STOC'01: Proceedings of the 33th Annual ACM Symposium on Theory of Computing*, July 6, 2001, Hersonissos, Greece, pp. 50–59
[5] Nielsen M A and Chuang I L 2000 *Quantum Computation and Quantum Information* (Cambridge: Cambridge University Press) pp. 248–271
[6] Jones J A, Mosca M and Hansen R H 1998 *Nature* **393** 344
[7] Kwiat P G, Mitchell J R, Schwindt P D D and White A G 2000 *J. Mod. Opt.* **47** 257
[8] Scully M O and Zubairy M S 2001 *Proc. Natl. Acad. Sci. USA* **98** 9490
[9] Dodd J L, Ralph T C and Milburn G J 2003 *Phys. Rev. A* **68** 042328

[10] Home J P, Hanneke D, Jost J D, Amini J M, Leibfried D and Wineland D J 2009 *Science* **325** 1227
[11] Childs A and Goldstone J 2004 *Phys. Rev. A* **70** 022314
[12] Manouchehri K and Wang J B 2014 *Physical Implementation of Quantum Walks* (Perth: The University of Western Australia) pp. 39–59
[13] Portugal R 2013 *Quantum Walks and Search Algorithms* (New York: Springer New York) pp. 17–37
[14] Abal G, Donangelo R, Marquezino F L and Portugal R 2010 *Math. Struct. Comput. Sci.* **20** 999
[15] Childs A, Farhi E and Gutmann S 2002 *Quantum Inf. Process.* **1** 35
[16] Childs A M, Cleve R, Deotto E, Farhi E, Gutmann S and Spielman D A 2003 *STOC'03: Proceedings of the 35th Annual ACM Symposiumon Theory of Computing*, June 9–11, 2003, San Diego, California, pp. 59–68
[17] Paparo G D and Martin-Delgado M A 2012 *Sci. Rep.* **2** 444
[18] Paparo G D, Muller M, Comellas F and Martin-Delgado M A 2014 *Eur. Phys. J. Plus* **129** 150
[19] Zhang H X, Chen T, Pan N Q and Zhang X D 2022 *Adv. Quantum Technol.* **5** 2270043
[20] Shenvi N, Kempe J and Whaley K B 2003 *Phys. Rev. A* **67** 052307
[21] Keating J P, Linden N, Matthews J C F and Winter A 2007 *Phys. Rev. A* **76** 012315
[22] Zhang Y, Bao W, Wang X and Fu X 2015 *Chin. Phys. B* **24** 080307
[23] Chen T and Zhang X D 2016 *Sci. Rep.* **6** 25767
[24] Chen T and Zhang X D 2016 *Phys. Rev. A* **94** 012316
[25] Niu R W and Pan G J 2016 *Chin. Phys. Lett.* **33** 68901
[26] Figgatt C, Maslov D, Landsman K A, Linke N M, Debnath S and Monroe C 2017 *Nat. Commun.* **8** 1918
[27] Lv L S, Zhang K, Zhang T and Ma M Y 2019 *Chin. Phys. B* **28** 020501
[28] Li T, Zhang S, Fu X Q, Wang X, Wang Y, Lin J and Bao W S 2019 *Chin. Phys. B* **28** 120301
[29] Zhang J, Hegde S S and Suter D 2020 *Phys. Rev. Lett.* **125** 030501
[30] Zhang R, Liu Y and Chen T 2020 *Phys. Rev. A* **102** 022218
[31] Qiang X G, Wang Y Z, Xue S C, Ge R Y, Chen L F, Liu Y W, Huang A Q, Fu X, Xu P, Yi T, Xu F F, Deng M T, Wang J B, Meinecke J D A, Matthews J C F, Cai X L, Yang X J and Wu J J 2021 *Sci. Adv.* **7** eabb8375
[32] Pan N Q, Chen T, Sun H J and Zhang X D 2021 *Research* **2021** 9793071
[33] Zhang R and Chen T 2022 *Commun. Theor. Phys.* **74** 045101
[34] Janmark J, Meyer D A and Wong T G 2014 *Phys. Rev. Lett.* **112** 210502
[35] Meyer D A and Wong T G 2015 *Phys. Rev. Lett.* **114** 110503
[36] Chakraborty S, Novo L, Ambainis A and Omar Y 2016 *Phys. Rev. Lett.* **116** 100501
[37] Wong T G and Meyer D A 2016 *Phys. Rev. A* **93** 062313
[38] Wong T G and Philipp P 2016 *Phys. Rev. A* **94** 022304
[39] Tulsi A 2016 *Quantum Inf. Process.* **15** 2675
[40] Wong T G 2016 *Quantum Inf. Process.* **15** 1411